$^{13}C-^{15}N$ Correlation via Unsymmetrical Indirect Covariance NMR: Application to Vinblastine

Gary E. Martin,*[,†] Bruce D. Hilton,[†] Kirill A. Blinov,[‡] and Antony J. Williams[§,⊥]

Schering-Plough Research Institute, Summit, New Jersey 07901, Advanced Chemistry Development, Moscow Division, Moscow, 117504, Russian Federation, and Advanced Chemistry Development, Toronto, Ontario M5C 1T4, Canada

Received July 24, 2007

Unsymmetrical indirect covariance processing methods allow the derivation of hyphenated 2D NMR data from the component 2D spectra, potentially circumventing the acquisition of the much lower sensitivity hyphenated 2D NMR experimental data. Calculation of HSQC-COSY and HSQC-NOESY spectra from GHSQC, COSY, and NOESY spectra, respectively, has been reported. The use of unsymmetrical indirect covariance processing has also been applied to the combination of $^{1}H-^{13}C$ GHSQC and $^{1}H-^{15}N$ long-range correlation data (GHMBC, IMPEACH, or CIGAR-HMBC). The application of unsymmetrical indirect covariance processing to spectra of vinblastine is now reported, specifically the algorithmic extraction of $^{13}C-^{15}N$ correlations via the unsymmetrical indirect covariance processing of the combination of $^{1}H-^{13}C$ GHSQC and long-range $^{1}H-^{15}N$ GHMBC to produce the equivalent of a $^{13}C-^{15}N$ HSQC-HMBC correlation spectrum. The elimination of artifact responses with aromatic solvent-induced shifts (ASIS) is shown in addition to a method of forecasting potential artifact responses through the indirect covariance processing of the GHSQC spectrum used in the unsymmetrical indirect covariance processing.

Long-range $^{1}H-^{15}N$ heteronuclear shift correlation NMR experiments at natural abundance have become progressively more important in natural product structure elucidation since the first reports appeared a little over a decade ago. There have been several reviews[1–5] and two recent publications that have described the simultaneous acquisition of $^{1}H-^{13}C$ and $^{1}H-^{15}N$ long-range heteronuclear chemical shift correlation spectra.[6,7] Recently, there has also been considerable interest in a relatively new area of investigation known as covariance NMR. A communication that described indirect covariance NMR processing of hyphenated HSQC-TOCSY data[8] spurred our interest in the potential capabilities of indirect covariance spectroscopy, which in turn led to the development of unsymmetrical indirect covariance NMR processing methods.[9] In an extension of our initial investigation, unsymmetrical indirect covariance NMR processing has been used to coprocess discretely acquired 2D NMR spectra to afford the equivalent of hyphenated 2D NMR spectra. Examples have included the coprocessing of GHSQC and GHMBC spectra to provide the equivalent of *m,n*-ADEQUATE spectra.[10] Coprocessing GHSQC and COSY spectra offers a covariance spectrum equivalent to a GHSQC-COSY spectrum.[11,12] GHSQC and NOESY spectra have also been coprocessed to afford correlation data equivalent to the very insensitive GHSQC-NOESY experiment.[13] Müller and co-workers[14] have also described the generation of $^{13}C-^{13}C$ correlation plots from HMBC spectra using covariance processing methods.

Carrying the utilization of unsymmetrical indirect covariance processing methods a step further, given two coherence transfer experiments of the type

$$A \rightarrow B \quad (1)$$

and

$$A \rightarrow C \quad (2)$$

it is possible to indirectly determine the coherence spectrum for

$$B \leftrightarrow C \quad (3)$$

Using this approach, we have recently shown that it is possible to mathematically combine $^{1}H-^{13}C$ GHSQC and long-range $^{1}H-^{15}N$ GHMBC or a similar long-range correlation experiment, e.g., IMPEACH-MBC or CIGAR-HMBC, to determine $^{13}C-^{15}N$ heteronuclear chemical shift correlation spectra.[15,16] In parallel work, Kupče and Freeman have shown it is possible to establish $^{13}C-^{15}N$ heteronuclear shift correlation using an unrelated technique known as projection reconstruction NMR.[7] We now wish to demonstrate the application of unsymmetrical indirect covariance processing methods to the mathematical combination of the $^{1}H-^{13}C$ GHSQC and long-range $^{1}H-^{15}N$ GHMBC spectra of vinblastine (**1**).

Table 1. Calculated (ACDLabs, Nitrogen NMR Chemical Shift Prediction Software, v10.2) versus Observed ^{15}N Chemical Shifts for Vinblastine (**1**)[a]

position	^{15}N HOSE code (ppm)	^{15}N neural network (ppm)	^{15}N observed (ppm)
N-1	66.0	66.7	64.1
N-9	55.3	56.0	67.0
N-6′	43.0	34.4	43.3
N-16′	138.2	138.9	136.0

[a] Observed data are taken from the 5 Hz optimized $^{1}H-^{15}N$ GHMBC assignments shown in Figure 1 and the spectrum shown in Figure 2.

Results and Discussion

Vinblastine, **1**, is a complex bis-indole alkaloid containing four ^{15}N resonances. The $^{1}H-^{15}N$ GHMBC spectrum of the alkaloid was acquired with the long-range delay optimized for 5 Hz, giving the correlations shown in the structure in Figure 1. The four nitrogen resonances were observed via long-range correlations to various protons at 43.3, 64.1, 67.0, and 136.0 ppm. The latter is readily assigned on the basis of its ^{15}N shift as the N-16′ indole nitrogen. ^{15}N chemical shifts for all of the nitrogens were calculated (ACD/Labs Nitrogen NMR chemical shift prediction software, v 10.2) using both HOSE-code and neural network calculations, which are summarized in Table 1. On the basis of the calculated ^{15}N chemical shifts, N-6′ was assigned as the ^{15}N resonance at 43.3 ppm. Long-range heteronuclear correlations were necessary to differentiate and assign unequivocally the nitrogen resonances at 64.1 and 67.0 ppm, as N-1 and N-9, respectively.

Figure 2 shows the $^{1}H-^{15}N$ GHMBC and multiplicity-edited $^{1}H-^{13}C$ GHSQC spectra flanking the $^{13}C-^{15}N$ HSQC-HMBC

* To whom correspondence should be addressed. Tel: +908.473-5398. Fax: +908.473-6559. E-mail: gary.martin@spcorp.com.
† Schering-Plough Research Institute.
‡ Advanced Chemistry Development, Moscow Division.
§ Advanced Chemistry Development, Toronto.
⊥ Present address: ChemZoo, Wake Forest, NC 27587.

10.1021/np070361t CCC: $37.00 © 2007 American Chemical Society and American Society of Pharmacognosy
Published on Web 11/29/2007

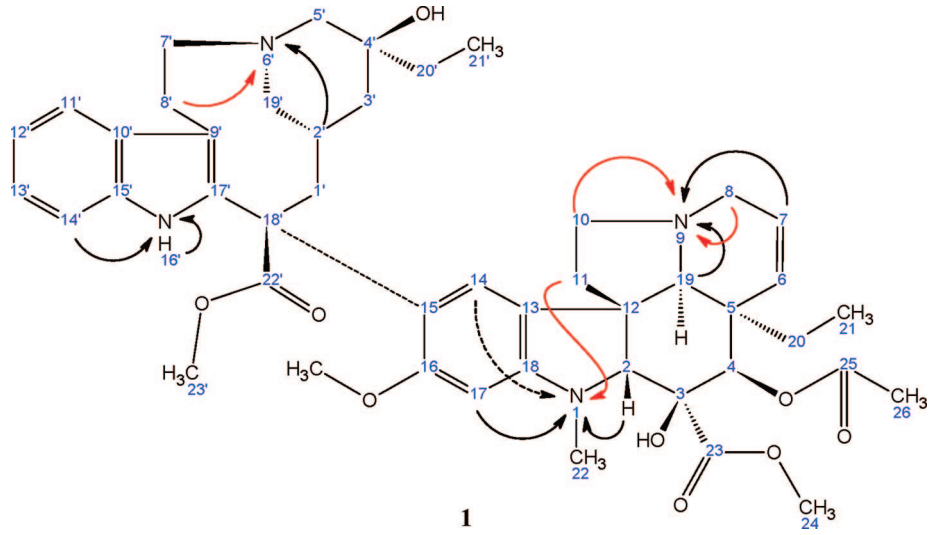

1

Figure 1. Structure of vinblastine (**1**) showing long-range $^{1}H-^{15}N$ correlations observed in the 5 Hz optimized $^{1}H-^{15}N$ GHMBC spectrum in d_6-DMSO at 26 °C. Dashed arrow denotes weak correlation. Red arrows are correlations from methylenes to ^{15}N and are color coded to correspond to responses from methylene carbons in the $^{13}C-^{15}N$ HSQC-HMBC spectrum shown in Figure 3. The NH correlation to N-16′ is not observed in the $^{13}C-^{15}N$ HSQC-HMBC spectrum since the H-16′ proton is not on a ^{13}C and the experiment did not sample $^{1}J_{NH}$ heteronuclear coupling information despite the fact that these correlations can be observed in a $^{1}H-^{15}N$ GHMBC or equivalent long-range heteronuclear shift correlation spectrum.

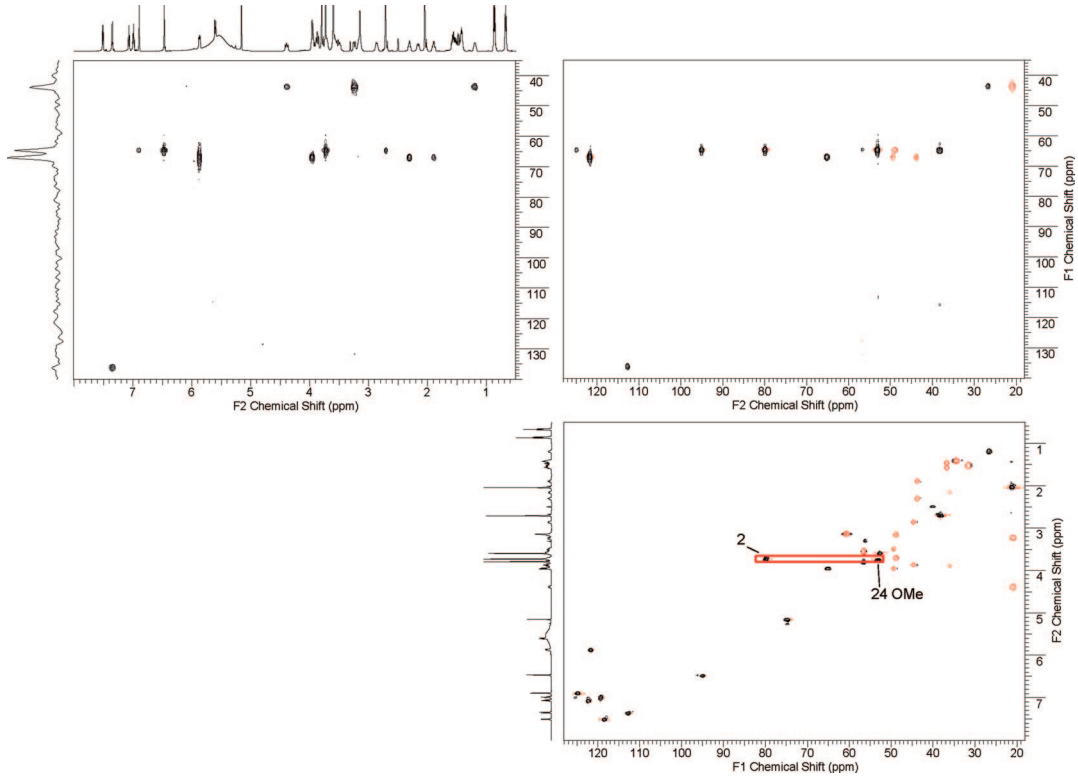

Figure 2. Composite plot showing the 5 Hz optimized $^{1}H-^{15}N$ GHMBC spectrum (top left panel) and the transposed, multiplicity-edited $^{1}H-^{13}C$ GHSQC (bottom right panel) spectra of vinblastine (**1**) used in the calculation of the $^{13}C-^{15}N$ HSQC-HMBC heteronuclear correlation spectrum shown in the top right panel. Methylene responses are inverted in the multiplicity-edited $^{1}H-^{13}C$ GHSQC spectrum and plotted in red; methine and methyl correlations have positive phase and are plotted in black. The carbon multiplicity information from the GHSQC spectrum is carried forward into the $^{13}C-^{15}N$ HSQC-HMBC spectrum. Methylene carbons correlated to ^{15}N appear in red; methine and methyl carbons correlated to ^{15}N are plotted in black. The fully annotated $^{13}C-^{15}N$ HSQC-HMBC correlation spectrum is shown in Figure 3.

correlation spectrum calculated using unsymmetrical indirect covariance processing. The GHSQC spectrum has been transposed to reflect the orientation of this spectrum used by the algorithm during the unsymmetrical indirect covariance processing, which gives ^{13}C chemical shift information in the F_2 dimension of the $^{13}C-^{15}N$ HSQC-HMBC correlation spectrum; ^{15}N chemical shift information is presented in the F_1 dimension of the spectrum. The fully assigned $^{13}C-^{15}N$ HSQC-HMBC spectrum is shown in Figure 3. With the sole exception of the apparent correlation response from the C-24 *O*-methyl resonance to N1, all of the responses are

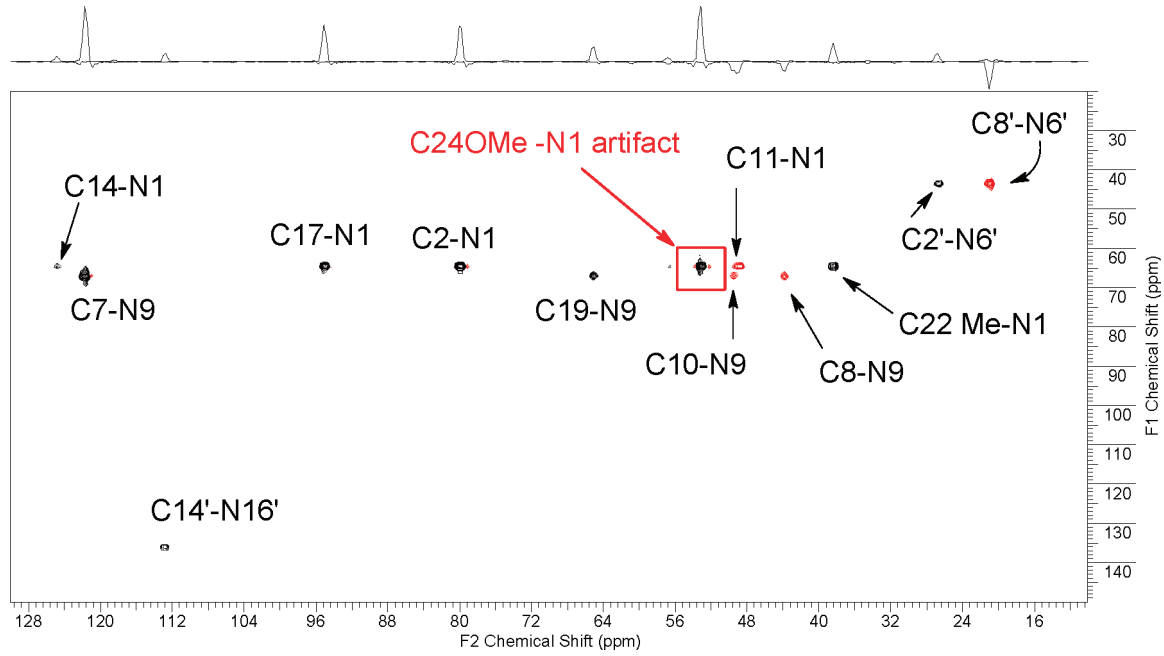

Figure 3. $^{13}C-^{15}N$ HSQC-HMBC spectrum from Figure 2 showing response assignments. The correlation response from the C24 *O*-methyl group to N-1 is obviously an artifact. Examination of the transposed, multiplicity-edited $^{1}H-^{13}C$ GHSQC panel in Figure 2 (red-boxed region, lower right panel) illustrates the overlap of the H-2 methine and the C24 *O*-methyl resonances. This type of overlap can give rise to artifact responses in unsymmetrical indirect covariance processed heteronuclear correlation data matrices.[8,9]

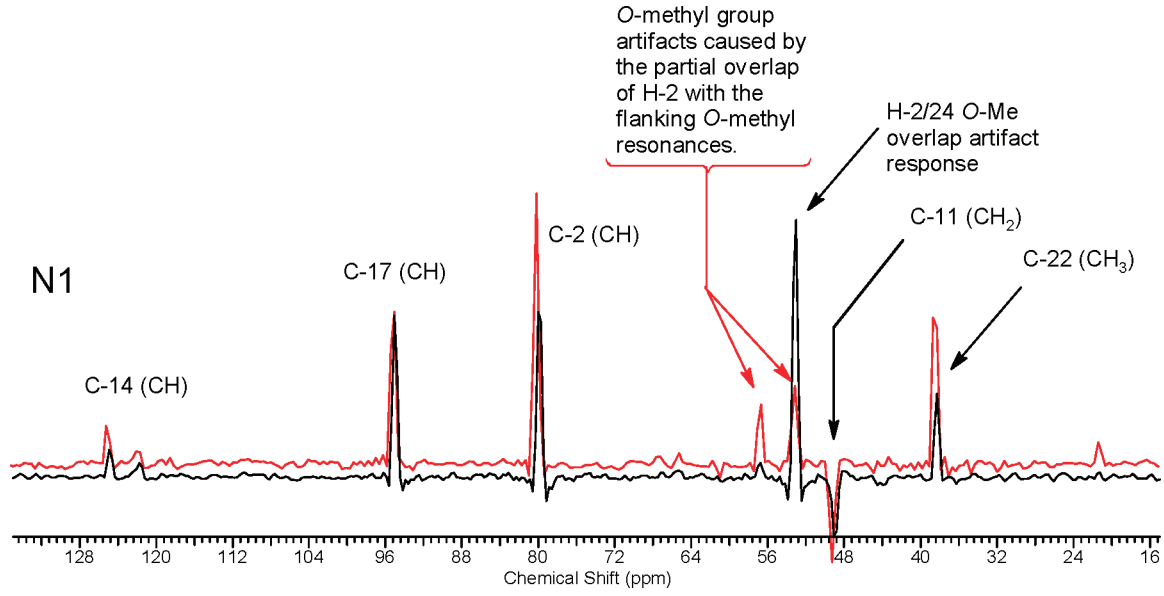

Figure 4. Slice at the N-1 chemical shift (64.1 ppm) from (black trace) the $^{13}C-^{15}N$ HSQC–HMBC spectrum in d_6-DMSO shown in Figures 2 and 3; slice from the $^{13}C-^{15}N$ HSQC-HMBC spectrum following the addition of 50 μL of d_6-benzene to the initial d_6-DMSO sample (red trace). The aromatic solvent-induced shift caused by the addition of d_6-benzene shifted the H-2 resonance slightly downfield between the C-16 and C-24 *O*-methyl resonances so that only the base of these resonances is overlapped in the 600 MHz ^{1}H spectrum (red trace). As a consequence of shifting the H-2 resonance, the C-24 *O*-methyl response went from being the largest response in the trace shown in the black trace to a much smaller response in the red trace. Simultaneously, the now slightly greater overlap of the base of the H-2 resonance and that of the C-16 *O*-methyl resonance led to some increase in the intensity of an artifact response for this resonance as would be expected with the increasing overlap of the pair of resonances.

reasonable (Figure 1). The apparent C-24 *O*-methyl correlation response arises because of an overlap of the H-2 methine and 24-*O*-methyl resonances in the ^{1}H spectrum (red-boxed region in the multiplicity-edited $^{1}H-^{13}C$ GHSQC spectrum shown in the bottom right panel of Figure 2; red-boxed response in the $^{13}C-^{15}N$ HSQC-HMBC spectrum shown in Figure 3).[8,9] As even partial overlap of the bases of Lorentzian peaks can potentially give rise to artifact responses, there is little likelihood that extensive linear prediction will eliminate artifact responses.[17]

To confirm the origin of the C-24 *O*-methyl-N-1 correlation response as an artifact, the 20 mg vinblastine sample used for this study was diluted by the addition of 50 μL of d_6-benzene, inducing an aromatic solvent-induced shift (ASIS) that shifted the H-2 resonance slightly downfield and between the 16- and 24-*O*-methyl

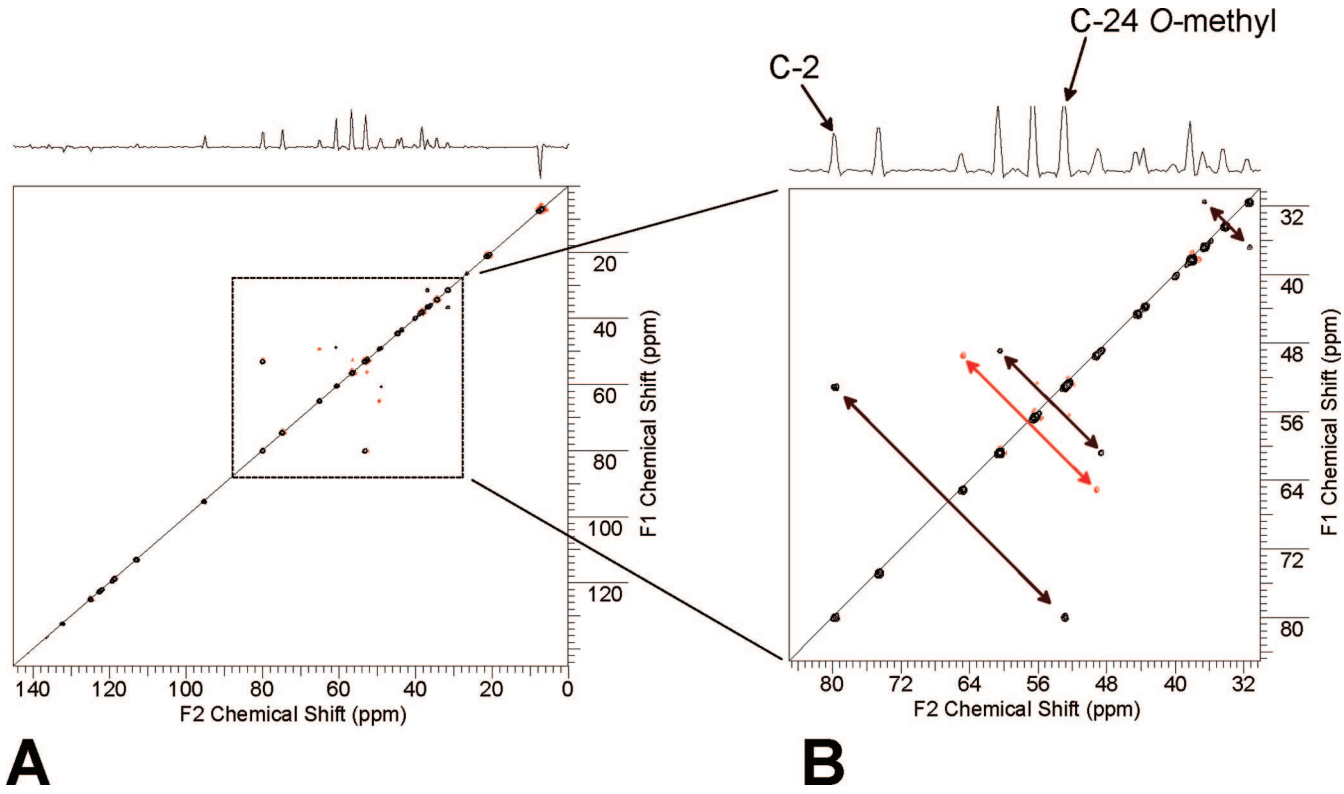

Figure 5. Panel A shows the conventional indirect covariance processed result from the multiplicity-edited GHSQC spectrum of vinblastine (**1**). Normally, this processing would not be done, as it does not provide useful correlation information. However, there are some correlation responses that need to be considered. Because of the nature of the indirect covariance processing algorithms, correlation responses in the indirect covariance processed result from a GHSQC spectrum can only occur due to resonance overlap. In the expansion shown in panel B the off-diagonal responses arising from the overlap of the H-2 and H-24 *O*-methyl resonances are labeled. Responses of this type are a predictor of potential artifact responses in the $^{13}C-^{15}N$ HSQC-HMBC correlation spectrum calculated by unsymmetrical indirect covariance processing shown in Figures 2 and 3. If one of the overlapped proton resonances exhibits a long-range correlation response to ^{15}N in the GHMBC spectrum used in the unsymmetrical indirect covariance processing, an artifact response can be observed at the corresponding ^{13}C chemical shift of the proton overlapped with the proton that is legitimately long-range correlated to ^{15}N. The artifact response will be observed at the ^{15}N shift of the nitrogen to which the legitimate correlation is observed. In the present case, H-2 is long-range coupled to N1, giving a correlation response for C-2−N-1 (Figure 3). The overlap of the H-2 and H-24 *O*-methyl resonances leads to a C-2−N-1 correlation response via the $^2J_{NH}$ correlation of H-2 to N-1 and consequently to the C-24−N-1 artifact response observed in Figure 3, as predicted in panel B.

singlets. Reacquisition of both the multiplicity-edited $^1H-^{13}C$ GHSQC and $^1H-^{15}N$ GHMBC spectra was followed again by unsymmetrical indirect covariance processing of the resulting 2D spectra. The N-1 slices at 64.1 from both $^{13}C-^{15}N$ HSQC-HMBC correlation spectra are shown in Figure 4.

The addition of the d_6-benzene to the sample provided an ASIS of the H-2 resonance downfield to a position between the flanking C-16 and C-24 *O*-methyl resonances. The C-24 *O*-methyl response was the most intense correlation response in the N-1 slice at 64.1 ppm, shown in Figure 4 by the black trace. When the H-2 resonance with which it was overlapped (Figure 2, GHSQC spectrum, lower right panel) was shifted downfield by the addition of d_6-benzene, the intensity of the C-24 *O*-methyl artifact response significantly diminished, as shown by the N-1 slice in Figure 4 by the red trace. Commensurate with the downfield shift of the H-2 resonance, the overlap of the bases of the Lorentzian lines for the H-2 and H-16 *O*-methyl resonance began to increase. The new H-16 *O*-methyl H-2 partial overlap caused an increase above the t_1 tracking noise at the shift of the C-16 *O*-methyl resonance in the black trace shown in Figure 4 to the level of the diminished C-24 *O*-methyl response in the red trace shown in Figure 4. These observations confirm that the response observed at the ^{13}C chemical shift of the C-24 *O*-methyl resonance in Figure 3 was indeed a consequence of the overlap of the H-2 and H-24 *O*-methyl resonances in the F_2 dimension of the $^1H-^{13}C$ GHSQC spectra used in the calculation of the $^{13}C-^{15}N$ HSQC-HMBC spectra.

A way of further enhancing the utility of $^{13}C-^{15}N$ HSQC-HMBC experiments without having to resort to further experimental work is available through the use of simple covariance processing. A GHSQC experiment would not normally be subjected to covariance processing, as there is no correlation information to be gained from this type of data manipulation. However, the specific case of a GHSQC spectrum with resonance overlaps of the type represented by the H-2 methine and H-24 *O*-methyl resonances may be considered. In this case, covariance processing of the GHSQC spectrum will give rise to a covariance spectrum in which the off-diagonal responses observed in the spectrum arise from proton resonance overlap. Figure 5A shows the result of covariance processing the GHSQC spectrum of vinblastine (**1**) prior to the addition of d_6-benzene. There are several sets of off-diagonal responses in the covariance spectrum, which is not surprising for a molecule of the complexity of **1**. The most prominent pair of off-diagonal responses were observed at the ^{13}C chemical shifts of the C-2 and C-24 *O*-methyl resonances. In this eventuality, if either of the pair of resonances with the off-diagonal responses has a directly bound proton that is long-range coupled to ^{15}N in the $^1H-^{15}N$ GHMBC spectrum, an artifact response can be anticipated at the ^{13}C chemical shift of the other member of the pair. In the case of vinblastine, there is a prominent C-2−N-1 correlation response, as expected. In addition, as has already been discussed, there is also a very strong artifact response at the C-24 ^{13}C and N-1 ^{15}N chemical shifts in the $^{13}C-^{15}N$ correlation spectrum shown

in Figure 3. Applying conventional covariance processing to the $^{1}H-^{13}C$ GHSQC spectrum of a molecule of interest prior to using unsymmetrical indirect covariance processing to generate a $^{13}C-^{15}N$ HSQC-HMBC heteronuclear shift correlation spectrum provides a convenient means of forecasting the possibility of artifact correlation responses in the unsymmetrical indirect covariance processed data. Furthermore, since a GHSQC spectrum will always be available when unsymmetrical indirect covariance processing is being done, the cost of this step is inconsequential and the interpretation of the covariance spectrum is a facile process.

As has been shown previously for simpler molecules,[15,16] multiplicity-edited $^{1}H-^{13}C$ GHSQC and $^{1}H-^{15}N$ long-range heteronuclear shift correlation spectra can be used successfully for unsymmetrical indirect covariance processing for molecules of the molecular complexity of vinblastine (**1**) with a relative minimum of artifacts. Further, by subjecting the initial multiplicity-edited $^{1}H-^{13}C$ GHSQC spectrum to covariance processing, the possibility of artifacts can be forecast on the basis of off-diagonal correlation responses in the covariance spectrum. We are currently exploring the potential benefits and impact of the availability of $^{13}C-^{15}N$ heteronuclear chemical shift correlation data on the computer-assisted structure elucidation of a group of model alkaloids, which will be the subject of a future report. We are also exploring the potential of covariance processing of GHSQC spectra for the prediction of artifacts in other unsymmetrical indirect covariance processing applications.

It should be noted that covariance[8,13] and unsymmetrical indirect covariance methods[10–13,15,16] do not create new connectivity information that is not already present in the spectra from which they are derived. Rather, these methods provide an alternative and potentially very efficient way to extract the connectivity information contained in the spectra being processed. In a sense, covariance processing methods are analogous to the Fourier transform. The interpretation of time domain data is essentially impossible, while the information content of a spectrum following conversion to the frequency domain is much more readily interpreted.

Experimental Section

General Experimental Procedures. A sample of 20 mg of vinblastine (**1**) (Sigma Aldrich) was prepared for NMR data acquisition by dissolving the material in ~180 μL of d_6-DMSO (CIL). The resulting solution was transferred to a 3 mm NMR tube (Wilmad) using a flexible Teflon needle and a gastight syringe (Hamilton). All NMR spectra were recorded using a Varian three-channel NMR spectrometer operating at a proton observation frequency of 599.75 MHz and equipped with a 5 mm Varian ColdProbe operating at an rf coil temperature of 20 K. The sample temperature was regulated at 26 °C. The GHSQC and GHMBC pulse sequences were used directly from the vendor-supplied pulse sequence library without modification. The one-bond delay in the HSQC experiment was optimized for 145 Hz. The long-range delay in the $^{1}H-^{15}N$ GHMBC experiment was optimized for 5 Hz. Gradient $^{1}H-^{13}C$ HSQC data were acquired, but nongradient data could be employed; gradient $^{1}H-^{15}N$ data are necessary to sufficiently flatten the noise floor of the 2D data matrix when data are acquired at natural abundance. The $^{1}H-^{13}C$ GHSQC data were acquired in ~30 min; the $^{1}H-^{15}N$ GHMBC data were acquired in 6.8 h. Spectral widths for both experiments in the F_2 frequency domain were 7225 Hz; F_1 spectral windows were optimized independently. All 2D NMR spectra were acquired with 1024 points in t_2 and were zero-filled to 2048 points prior to the first Fourier transform. The second frequency domain of both experiments was digitized using 128 increments of the evolution time, t_1, after which the data were linear predicted to 256 points and then zero-filled to 512 points prior to the second Fourier transform. The $^{1}H-^{13}C$ GHSQC spectrum was acquired with 8 transients/t_1 increment. The $^{1}H-^{15}N$ GHMBC data were acquired with 128 transients/t_1 increment. All NMR data processing was done using the ACD/Labs SpecManager v10.02 software. Unsymmetrical indirect covariance calculations took ~4 s using a laptop computer with 1 Gbyte of RAM and a 1.8 GHz processor. For the ASIS experiments, 50 μL of d_6-benzene (CIL) was added to the sample.

References and Notes

(1) Martin, G. E.; Hadden, C. E. *J. Nat. Prod.* **2000**, *65*, 543–585.
(2) Marek, R.; Lycka, A. *Curr. Org. Chem.* **2002**, *6*, 35–66.
(3) Martin, G. E.; Williams, A. J. *Annu. Rep. NMR Spectrosc.* Webb, G. A., Ed.; Elsevier: Amsterdam, 2005; Vol. 18, pp 1–119.
(4) Forgo, P.; Homann, J.; Dombi, G.; Máthé, L. In *Poisonous Plants and Related Toxins*; Acamovic, T., Steward, S., Pennycott, T. W., Eds.; CABI Publishing: Wallingford, UK, 2004; pp 322–328.
(5) Martin, G. E.; Solntseva, M.; Williams, A. J. In *Modern Alkaloids*,, Fattorusso, E., Taglialatela-Scafati, O., Eds.; Wiley-VCH: New York, 2007, in press.
(6) Pérez-Trujillo, M.; Nolis, P.; Parella, T. *Org. Lett.* **2007**, *9*, 29–32.
(7) Kupče, E.; Freeman, R. *Magn. Reson. Chem.* **2007**, *45*, 103–105.
(8) Zhang, Z.; Brüschweiler, R. *J. Am. Chem. Soc.* **2004**, *126*, 13180–13181.
(9) Blinov, K. A.; Larin, N. I.; Kvasha, M. P.; Moser, A.; Williams, A. J.; Martin, G. E. *Magn. Reson. Chem.* **2005**, *43*, 999–1007.
(10) Blinov, K. A.; Larin, N. I.; Williams, A. J.; Zell, M.; Martin, G. E. *Magn. Reson. Chem.* **2006**, *44*, 107–109.
(11) Blinov, K. A.; Larin, N. I.; Williams, A. J.; Mills, K. A.; Martin, G. E. *J. Heterocycl. Chem.* **2006**, *43*, 163–166.
(12) Martin, G. E.; Hilton, B. D.; Irish, P. A.; Blinov, K. A.; Williams, A. J. *J. Nat. Prod.* **2007**, *70*, 1393–1397.
(13) Blinov, K. A.; Williams, A. J.; Hilton, B. D.; Irish, P. A.; Martin, G. E. *Magn. Reson. Chem.* **2007**, *45*, 544–546.
(14) Schoeflberger, W.; Smrečki, V.; Vikić-Topić, D.; Müller, N. *Magn. Reson. Chem.* **2007**, *45*, 583–589.
(15) Martin, G. E.; Hilton, B. D.; Irish, P. A.; Blinov, K. A.; Williams, A. J. *Magn. Reson. Chem.* **2007**, *45*, 624–627.
(16) Martin, G. E.; Hilton, B. D.; Irish, P. A.; Blinov, K. A.; Williams, A. J. *J. Heterocycl. Chem.* **2007**, *44*, 1219–1222.
(17) Martin, G. E.; Hilton, B. D.; Blinov, K. A.; Williams, A. J. *Magn. Reson. Chem.* **2008**, in press.

NP070361T